Anal. Chem. **2002,** *74,* 2547−2555

Characterization of a Cross-Reactive Electronic Nose with Vapoluminescent Array Elements

Steven M. Drew,† Daron E. Janzen, and Kent R. Mann*

Department of Chemistry, University of Minnesota, Minneapolis, Minnesota 55455

A three-channel cross-reactive sensor array based on vapoluminescent platinum(II) double salt materials has been characterized. Two arrays were studied, one consisting of [Pt(CN-cyclododecyl)$_4$][Pt(CN)$_4$] (1), [(phen)Pt(CN-cyclohexyl)$_2$][Pt(CN)$_4$] (2), and [Pt(CN-*n*-tetradecyl)$_4$][Pt(CN)$_4$] (3) materials, where phen = 1,10-phenanthroline, and a second array that has compound 3 replaced by the mixed double salt material [(phen)Pt(CN-cyclododecyl)Cl)]$_2$[(phen)Pt(CN-cyclododecyl)$_2$]$_2$[Pt(CN)$_4$]$_3$ (4). Compounds 2, 3 and 4 are characterized here for the first time. Inclusion of solvent vapors into these materials often leads to dramatic shifts in their solid-state absorption and luminescence spectra. In these studies the arrays were exposed to a set of 10 test solvent vapors to determine the ability of each cross-reactive array to give reproducible vapoluminescent spectra characteristic of each solvent vapor. It was discovered that temperature programming between solvent vapor exposures greatly improved the reproducibility of the luminescence spectra obtained. A statistical analysis of three-dimensional resolution factors between pairs of solvent clusters in principal component space supported this assertion. The success of the temperature programming protocol was limited by the thermal stability and the sensitivity to low background water vapor levels of some platinum(II) double salt materials. The ability of the cross-reactive sensor array to differentiate between two different solvent vapors over a large concentration range was also investigated. Acetone and methanol were found to occupy two distinct regions of the three-dimensional principal component space. Detection limits for acetone and methanol were estimated from the principal component analysis as 75 and 6 g/m^3, respectively.

The development of cross-reactive arrays for gas sensing continues to be an active area of research. The goal of many investigators in this area is the development of a practical "electronic nose".[1] Gardner and Bartlett define an electronic nose as "an instrument which comprises an array of electronic chemical sensors with partial specificity and an appropriate pattern recognition system, capable of recognizing simple or complex odors."[2] The development and characterization of new cross-reactive transducer materials is critical if electronic nose sensors are to be applied in practical analytical measurements. Many types of transducer materials for cross-reactive arrays have been investigated including the following: semiconducting metal oxides,[1b,3] conducting polymer films,[4] acoustic wave devices,[5] field-effect transistors,[6] carbon black-loaded polymer film chemoresistors,[7] and conductometric sensors based on electrolyte/polymer composites.[8] Optical transducers also show great promise as cross-reactive sensor arrays. Some examples include the immobilization of dyes such as Nile Red[9] and metalloporphyrins[10] on chemically modified porous silica microspheres or surface-modified photoluminescent semiconductor materials.[11]

Our previous studies[12] suggested that pure vapochromic and vapoluminescent compounds[13] could be used in the solid state as optical transducers. Vapochromism in crystalline [Pt(CNR)$_4$][Pt(CN)$_4$] salts arises from highly anisotropic packing forces that enable solvent vapors to reversibly penetrate the interior of the material to form a new crystalline phase with precisely determined solvent−chromophore interactions.[12] These include changes in the dielectric constant near the chromophore, hydrogen bonding

† Current address: Department of Chemistry, Carleton College, Northfield, Minnesota 55057.

(1) (a) Gardner, J. W.; Bartlett, P. N. *Electronic Noses: Principles and Applications*, Oxford University Press: New York, 1999. (b) Persaud, K.; Dodd, G. H. *Nature (London)* **1982**, *299*, 352. (c) Albert, K. J.; Lewis, N. S.; Schauer, C. L.; Sotzing, G. A.; Stitzel, S. E.; Vaid, T. P.; Walt, D. R. *Chem. Rev.* **2000**, *100*, 2595−2626.

(2) Gardner, J. W.; Bartlett, P. N. *Sens. Actuators, B* **1994**, *18*−*19*, 211.

(3) Gardner, J. W.; Pike, A.; de Rooij, N. F.; Koudelka-Hep, M.; Clerc, P. A.; Hierlemann, A. *Sens. Actuators, B* **1995**, *26*, 135−139.

(4) (a) Bartlett, P. N.; Archer, P. B. M.; Ling-Chung, S. K. *Sens. Actuators* **1989**, *19*, 125−140. (b) Pearce, T. C.; Gardner, J. W.; Friel, S.; Bartlett, P. N.; Blair, N. *Analyst* **1993**, *118*, 371−377.

(5) (a) Grate, J. W. *Chem. Rev.* **2000**, *100*, 2627−2648. (b) Grate, J. W.; Zellers, E. T. *Anal. Chem.* **2000**, *72*, 2861−2868.

(6) Lundstrom, I.; Hedborg, E.; Spetz, A.; Sundgren, H.; Winquist, F. Electronic Nose Based on Field Effect Structures. In *Sensors and Sensory Systems for an Electronic Nose*; Gardner, J. W., Bartlett, P. N., Eds.; NATO ASI Series 212; Kluwer: Dordrecht, The Netherlands, 1992; pp 303−319.

(7) (a) Lonergan, M. C.; Severin, E. J.; Doleman, B. J.; Beader, S. A.; Grubbs, R. H.; Lewis, N. S. *Chem. Mater.* **1996**, *8*, 2298−2312. (b) Sotzing, G. A.; Briglin, S. M.; Grubbs, R. H.; Lewis, N. S. *Anal. Chem.* **2000**, *72*, 3181−3190. (c) Doleman, B. J.; Lewis, N. S. *Sens. Actuators, B* **2001**, *72*, 41−50.

(8) (a) Miller, L. L.; Boyd, D. C.; Schmidt, A. J.; Nitzkowski, S. C.; Rigaut, S. *Chem. Mater.* **2001**, *13*, 9−11. (b) Miller, L. L.; Bankers, J. S.; Schmidt, A. J.; Boyd, D. C. *J. Phys. Org. Chem.* **2000**, *13*, 808−815.

(9) (a) Dickinson, T. A.; White, J.; Kauer, J. S.; Walt, D. R. *Nature* **1996**, *382*, 697−700. (b) Michael, K. L; Taylor, L. C.; Schultz, S. L.; Walt, D. R. *Anal. Chem.* **1998**, *70*, 1242. (c) Dickinson, T. A.; Michael, K. L.; Kauer, J. S.;.; Walt, D. R. *Anal. Chem.* **1999**, *71*, 2192. (d) Albert, K. J.; Walt, D. R.; Gill, D. S.; Pearce, T. C. *Anal. Chem.* **2001**, *73*, 2501−2508.

(10) (a) Rakow, N. A.; Suslick, K. S. *Nature* **2000**, *406*, 710−713. (b) Di Natale, C.; Salimbeni, D.; Paolesse, R.; Macagnano, A.; D'Amico, A. *Sens. Actuators, B* **2000**, *65*, 220−226.

(11) (a) Seker, F.; Meeker, K.; Kuech, T. F.; Ellis, A. B. *Chem. Rev.* **2000**, *100*, 2505−2536. (b) Ivanisevic, A.; Ellis, A. B.; Ashkenasy, G.; Shanzer, A.; Rosenwaks, Y. *Langmuir* **2000**, *16*, 7852−7858. (c) Sohn, H.; Letant, S.; Sailor, M. J.; Trogler, W. C. J. *Am. Chem. Soc.* **2000**, *122*, 5399−5400.

10.1021/ac011255d CCC: $22.00
Published on Web 04/26/2002

Chart 1

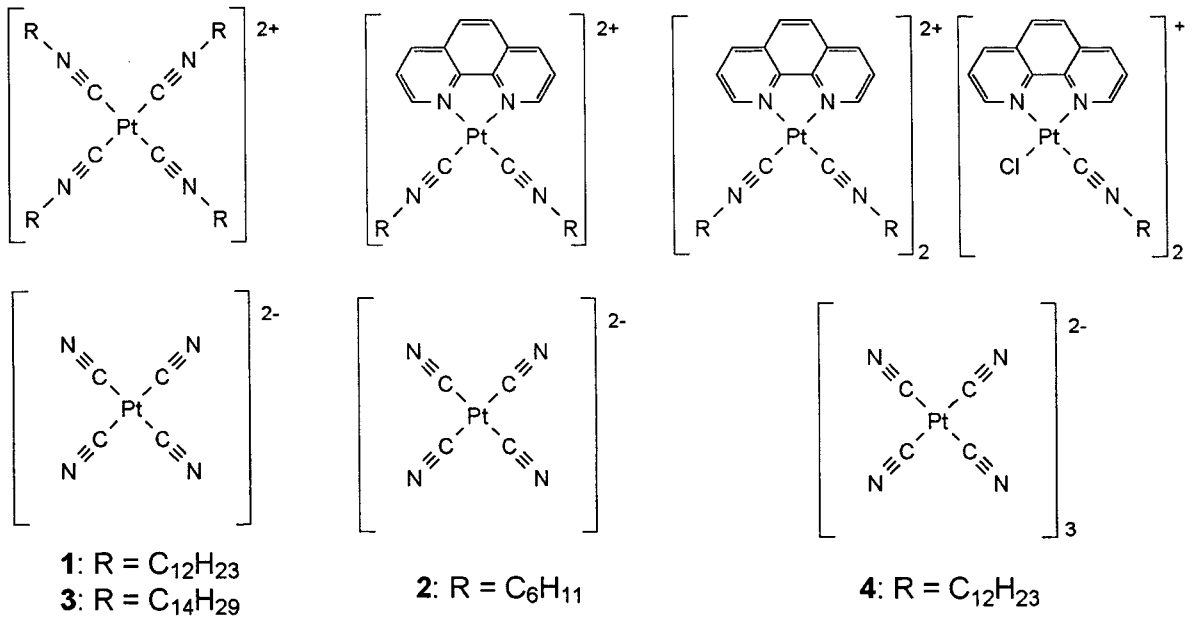

between the solvent and coordinated cyanide, and expansion or contraction of the unit cell that is coupled to the Pt−Pt distance.[12] The $[Pt(CNR)_4][Pt(CN)_4]$ solids consist of infinite stacks of alternating $[Pt(CNR)_4^{2+}]$ dications and $[Pt(CN)_4^{2-}]$ dianions. Interionic metal−metal interactions produce the chromophore.[12] The vapor inclusion causes color changes that result from a combination of chemical interactions with the chromophore including changes in the dielectric constant near the chromophore, hydrogen bonding between the solvent and coordinated cyanide, and expansion or contraction of the unit cell that is coupled to changes in the Pt−Pt distance.

In an earlier communication,[14] we reported on initial findings with an array of three new vapoluminescent salts (see Chart 1): $[Pt(CN\text{-cyclododecyl})_4][Pt(CN)_4]$ (**1**), $[(phen)Pt(CN\text{-cyclohexyl})_2][Pt(CN)_4]$ (**2**), and $[Pt(CN\text{-}n\text{-tetradecyl})_4][Pt(CN)_4]$ (**3**), where phen = 1,10-phenanthroline. Since that communication, we have also investigated an additional vapoluminescent salt, specifically, $[(phen)Pt(CN\text{-cyclododecyl})Cl)]_2[(phen)Pt(CN\text{-cyclododecyl})_2]_2[Pt(CN)_4]_3$ (**4**), (see Chart 1). In this paper, we report additional data that address the reversibility, stability, and sensing characteristics of these vapoluminescent materials for potential electronic nose analytical applications.

EXPERIMENTAL SECTION

General Considerations. The details for the synthesis and characterization of **1**−**4**, the isocyanide ligands, and the ligand precursors (formamides) are given in the Supporting Information or were previously reported.[12] The solvents used to generate solvent vapors (acetone, cyclohexane, benzene, chloroform, 2-propanol, 1-propanol, ethanol, methanol, water, dichloromethane) were all of spectral grade or better. Nitrogen gas saturated with solvent vapors was generated by slowly bubbling compressed nitrogen through a flask, submerged in a room-temperature water bath, containing the liquid solvent of interest. For most experiments, no attempt was made to "dry" the compressed nitrogen gas (industrial grade) used to carry solvent vapors into the three-channel sensor unless otherwise noted. "Dry" nitrogen gas, when used, was generated from the bleed of a liquid nitrogen dewar. Solvent vapors were assumed to be saturated in the nitrogen stream. This corresponds to the following concentrations (in g/m^3): acetone (620), cyclohexane (380), benzene (300), chloroform (1100), 2-propanol (130), 1-propanol (64), ethanol (130), methanol (200), water (23), and dichloromethane (2000). Dilution of the saturated vapor streams of acetone and methanol was carried out with a partitioned flow system. The partitioned gas flow system was constructed using mass flow controllers and solenoid valves under computer control. Specifically, a 0−10 SSCM mass flow controller (Omega FMA 1400) passed nitrogen gas through a glass bubbler containing the solvent of interest. The flow of nitrogen saturated with solvent vapor was teed into the flow of a diluting nitrogen gas stream regulated by either a 0−10 or a 0−50 SCCM mass flow controller. A PC equipped with LabVIEW (National Instruments) controlled the mixing of the saturated vapor stream with the diluting nitrogen gas stream. Percentages available ranged from 100 (pure saturated vapor, no diluting nitrogen gas) to 0% (no saturated vapor, pure diluting nitrogen gas). Percentages between 0 and 100% were corrected for the expansion that occurs when the nitrogen gas flowing through the solvent bubbler picks up solvent vapor, thus increasing the flow rate of the solvent-saturated stream above the setting of the mass flow valve feeding nitrogen into the solvent bubbler. For clarity, the percentages listed in Figure 7 are uncorrected values. The details of this correction and a table of corrected values

(12) (a) Exstrom, C. L.; Sowa Jr., J. R.; Daws, C. A.; Janzen, D.; Moore, G. A.; Stewart, F. F.; Mann, K. R. *Chem. Mater.* **1995**, *7*, 15−17. (b) Daws, C. A.; Exstrom, C. L.; Sowa Jr., J. R.; Mann, K. R *Chem. Mater.* **1997**, *9*, 363−368. (c) Exstrom, C. L.; Pomije, M. K.; Mann, K. R. *Chem. Mater.* **1998**, *10*, 942−945. (d) Buss, C. E.; Anderson, C. E.; Pomije, M. K.; Lutz, C. M.; Britton, D.; Mann, K. R. *J. Am. Chem. Soc.* **1998**, *120*, 7783−7790. (e) Buss, C. E.; Mann, K. R. *J. Am. Chem. Soc.* **2002**, *124*, ASAP. (f) Grate, J. W.; Moore, L. K.; Janzen, D. E.; Veltkamp, D. J.; Kaganove, S.; Drew, S. M.; Mann, K. R. *Chem. Mater.* **2002**, *14*, 1058−1066.

(13) (a) Cariati, E.; Bu, X.; Ford, P. C. *Chem. Mater.* **2000**, *12*, 3385−3391. (b) Beauvais, L. G.; Shores, M. P.; Long, J. R. *J. Am. Chem. Soc.* **2000**, *122*, 2763−2772. (c) Mansour, M. A.; Connick, W. B.; Lachicotte, R. J.; Gysling, H. J.; Eisenberg, R. *J. Am. Chem. Soc.* **1998**, *120*, 1329−1330.

(14) Drew, S. M.; Janzen, D. E.; Buss, C. E.; MacEwan, D. I.; Dublin, K. M.; Mann, K. R. *J. Am. Chem. Soc.* **2001**, *123*, 8414−8415.

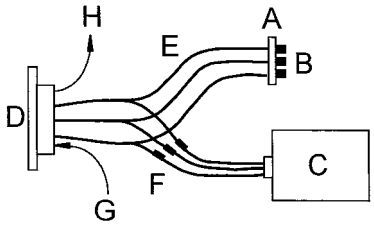

Figure 1. Schematic of three-channel vapoluminescence sensor: (A) Band-pass filter, 436 nm; (B) blue diodes; (C) CCD spectrophotometer; (D) three-channel sample holder and vapor flow cell; (E) bifurcated fiber optics; (F) filter holder; (G) solvent vapor flow in; (H) solvent vapor flow out.

for the methanol and acetone concentrations are included in the Supporting Information.

Three-Channel Vapoluminescence Sensor. A three-channel vapoluminescence sensor was constructed using the following components: a set of blue light-emitting diodes (Radio Shack, λ_{max} = 468 nm), bifurcated fiber optics (Edmond Scientific), a three-channel sensor gas flow cell (constructed in-house), and a 256 × 1024 CCD spectrophotometer (Princeton Instruments). A schematic diagram of the apparatus is depicted in Figure 1. The blue diodes were mounted on one side of a 436-nm band-pass filter and monochromatic excitation light was collected by three fiber-optic cables mounted on the opposite side. The excitation light entered the three-channel sensor gas flow cell through three bifurcated fiber-optic cables that also collected the luminescence from the sensor compounds and passed it on to the CCD camera. The gas flow cell was constructed by mounting the three bifurcated fiber-optic cables in a plate that could be positioned above three wells that comprise the three channels of the sensor. For experiments that did not require heating of the sensor compounds, the compounds were deposited from a diethyl ether suspension into each well. The amount of sensor compound deposited ranged from 0.5 to <0.1 mg. For experiments that required a heating cycle, the sensor compounds were deposited onto a flexible, foil heater (Minco) or a set of thermistors (DigiKey) that were designed to heat to a specific temperature (50, 80, 100 °C). The temperature of the heating device was monitored by mounting a thermocouple in the cell. A space between the plate with the mounted fiber optics and the plate holding the sensor compound was maintained with a Teflon gasket. A nitrogen stream carrying solvent vapors was passed through this space. The luminescence collected by the three bifurcated fiber optics was passed though an in-line filter to remove any reflected excitation light. The ends of the three fibers were mounted in a vertical line on a disk that was mounted at the entrance slit to the CCD camera. The luminescence from the three fibers was used to position the disk so that an image of three distinct luminescence spectra, one for each channel of the sensor array, could be acquired simultaneously. The three spectra obtained were binned, and dark current was subtracted on-line.

Principal Component Analysis. The binned luminescence spectra acquired for each channel of the sensor were normalized to the maximum intensity found on each channel and mean centered before assembling the data into a matrix for principal component analysis (PCA).[15] PCA was based on the covariance matrix of the raw spectral data. Typically, 46 points were used from each channel, for a total of 138 data points describing each solvent vapor in the raw spectral data matrix. The first three scores of the PCA usually described greater than 90% of the variance in the data set. See Supporting Information for loadings plots and PC3 versus PC1 plots associated with all PCA calculations reported. Differentiation of the solvent clusters in PC space was quantified with a form of linear discrimination similar to that used by Lewis et al.[7] In short, the distance in PC space between solvent clusters was described in a pairwise manner. First, a vector ($\vec{w}$), which passes through the three-dimensional centroids of two adjacent clusters (a and b), was defined and the distance between the two centroids ($d_{\vec{w}}$) was calculated. Next, the PC coordinates of the two solvent clusters were projected onto the one-dimensional distance vector and a standard deviation for each cluster was calculated ($\sigma_{a,\vec{w}}$ and $\sigma_{b,\vec{w}}$). A resolution factor (rf) was then defined and calculated with eq 1.

$$\mathrm{rf} = d_{\vec{w}} / \sqrt{\sigma_{a,\vec{w}}^2 + \sigma_{b,\vec{w}}^2} \qquad (1)$$

Placing the constraint of a Gaussian distribution on the data set allows the overlap between the two clusters to be determined. In general, if two adjacent clusters have similar standard deviations when projected onto their distance vector, an rf value of 3.75 or greater implies less than 1% overlap between the two Gaussian curves.

RESULTS AND DISCUSSION

Transducer Materials. The pure cation platinum(II) double salt materials synthesized for this study (**1**−**3**) were synthesized and characterized using methods we have previously reported.[12] All three materials were synthesized by reacting $[(n\text{-}C_4H_9)_4N]_2[Pt(CN)_4]$ with solutions of $[Pt(C_{12}H_{23}{-}NC)_4]^{2+}$, $[(phen)Pt(C_6H_{11}{-}NC)_2]^{2+}$, or $[Pt(C_{14}H_{29}{-}NC)_4]^{2+}$ in acetonitrile to give **1**−**3**, respectively. Compounds **1**−**3** were all highly colored and gave the expected IR spectra and elemental analyses. Compound **4** is a mixed cation platinum(II) double salt, the likes of which we have not previously reported. In this case, the reaction of the starting material $[(phen)Pt(DMSO)Cl)]^+$ with $C_{12}H_{23}{-}NC$ at a 1:2 stoichiometry consistently led to the formation of a 1:1 mixture of platinum(II) cations: $[(phen)Pt(C_{12}H_{23}{-}NC)Cl]^+$ and $[(phen)Pt(C_{12}H_{23}{-}NC)_2]^{2+}$. Addition of $[(n\text{-}C_4H_9)_4N]_2[Pt(CN)_4]$ to the solution of cations precipitated a double salt with a reproducible mixture of +1 and +2 cations, $[(phen)Pt(CN\text{-}cyclododecyl)Cl)]_2[(phen)Pt(CN\text{-}cyclododecyl)_2]_2[Pt(CN)_4]_3$, as evidenced by the elemental analysis and spectroscopic characterizations. Additional evidence for the formulation of **4** as $[(phen)Pt(CN\text{-}cyclododecyl)Cl)]_2[(phen)Pt(CN\text{-}cyclododecyl)_2]_2[Pt(CN)_4]_3$ is provided in the Supporting Information.

Sensor Array Characterization. As we previously described,[14] arrays of platinum(II) double salt compounds produce luminescence spectra that depend on the solvent vapor in contact with the compounds. When these spectra were analyzed by PCA, distinct clusters representing various solvent vapors were obtained. It was reported that exposure of the array to nitrogen gas saturated with acetone vapor between analyte solvent vapor exposures seemed to improve the reversibility and reproducibility

(15) (a) Jurs, P. C.; Bakken, G. A.; McClelland, H. E. *Chem. Rev.* **2000**, *100*, 2649−2678. (b) Jackson, J. E. *A User's Guide to Principal Components*; Wiley and Sons: New York, 1991.

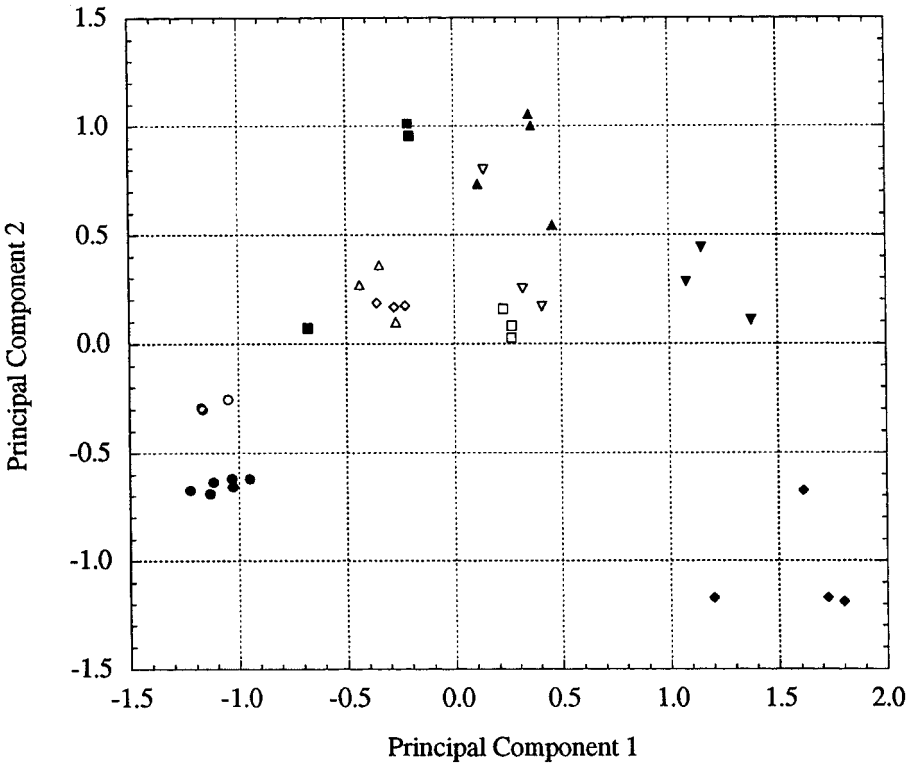

Figure 2. PC2 vs PC1 score plot of luminescence spectra acquired with array **I** with intervening acetone exposures ($T = 22$ °C). Individual percent variances: PC1 48; PC2 24. Solvent vapors: acetone (●), 1-propanol (□), 2-propanol (◇), benzene (△), cyclohexane (○), chloroform (■), dichloromethane (◆), water (▲), methanol (▼), and ethanol (▽).

of the array response;[14] however, this was not totally effective as certain solvent vapor exposure sequences still gave irreproducible spectra.[14] Temperature programming between solvent vapor exposures, i.e., a regulated ramped heating and cooling cycle of the array elements in the presence of nitrogen gas, was found to be much more effective. Figures 2 and 3 provide a comparison of the effects of acetone vapor exposure relative to temperature programming on the discrimination power of an array consisting of **1**−**3**, which will be referred to as array **I**. Tables 1 and 2 provide the rf values for the 45 solvent cluster pairs in Figures 2 and 3, respectively. Statistical analysis of the rf tables showed that the intervening acetone exposure gave a set of rf values with a mean of 6.3, a minimum of 0.51, and a maximum of 17. In addition, 13 of the rf values out of the 45 solvent vapor pairs were less than 3.75. In general, an rf value of less than 3.75 indicates a greater than 1% overlap and therefore relatively poor discrimination between the two solvents. When intervening temperature programming was introduced, the mean increased to 13, with a minimum rf of 1.4 and a maximum rf of 41. The number of rf values less than 3.75 decreased to 5 out of the 45 solvent vapor pairs; however, the resolution between several pairs decreased, especially some involving benzene vapor (vide infra). Obviously, temperature programming improved the average discrimination ability of the array and merited further investigation.

Several experiments were performed to optimize the effectiveness of temperature programming. For the first set of experiments, array **I** was used in the three-channel vapoluminescent sensor. For experiments involving temperature programming, **1** and **2** were deposited on the surface of thermistors mounted in the array flow cell. Compound **3** was found to decompose when heated much above room temperature, so it was deposited into an unheated well in the array flow cell. Four temperatures were chosen for study: 25, 50, 80, and 100 °C. After a round of solvent exposure and acquisition of the associated luminescence spectra (2−3 min.), the gas flow was switched to pure compressed nitrogen. For the room-temperature studies, the nitrogen flow was maintained for 4−5 min before the next solvent vapor exposure occurred. The cycle time is more a function of the thermal time constant and dead volume of the cell rather than the intrinsic response time of the array, which is on the order of 10 s or less for most vapors. To achieve higher temperatures between solvent vapor exposures, a voltage (15 V dc) was placed across the thermistors, which quickly (<30 s) heated them to their prescribed temperature maximums. The temperature maximum was held for an additional 30 s, after which the voltage difference was discontinued and the thermistors were allowed to cool back to room temperature (25 ± 1 °C). The cooling time was determined by the maximum temperature and ranged from ∼3 min for a 50 °C temperature maximum to greater than 7 min for a 100 °C temperature maximum. When room temperature was reestablished in the sensor cell a "background" nitrogen spectrum was acquired. Next, the nitrogen flow was diverted through a solvent, creating a nitrogen stream saturated with solvent vapor. A new luminescence spectrum was established very quickly, usually in less than 30 s. This luminescence spectrum was also recorded at 25 ± 1 °C. The array of luminescence spectra acquired for each solvent vapor at each temperature was examined by PCA followed by an rf calculation involving all the possible solvent pairs in PC space. The results of these experiments are described in Table 3. The data in Table 3 reveal a definite improvement in the ability

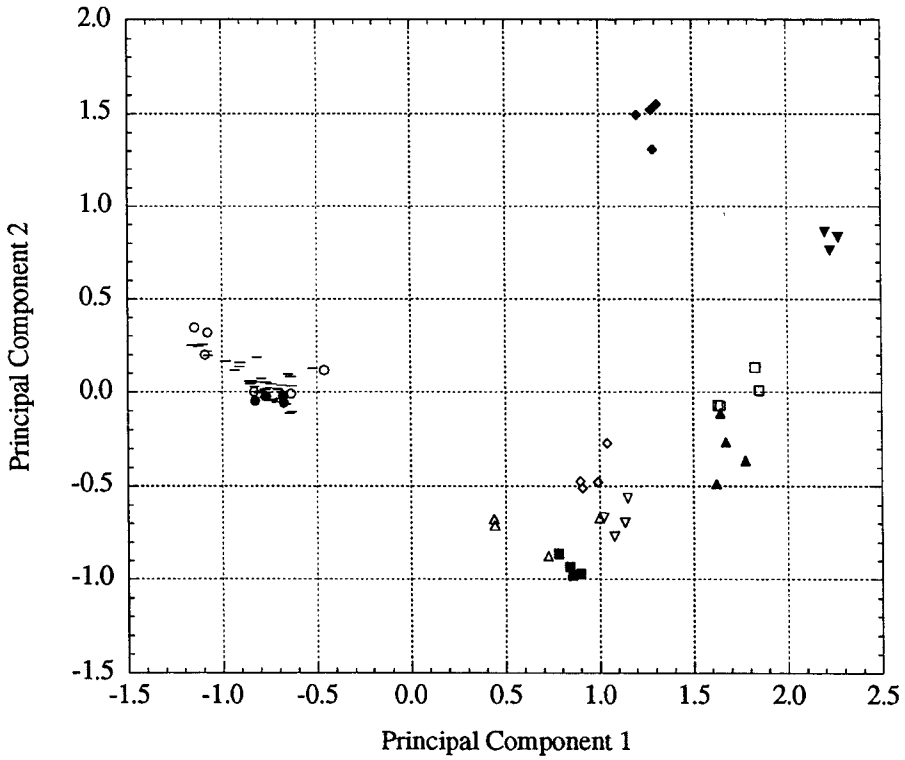

Figure 3. PC2 vs PC1 score plot of luminescence spectra acquired with array **I** with intervening temperature programming under nitrogen. Only **1** and **2** are directly heated by ramping up to 80 °C and then cooling to 25 ± 1 °C before acquiring spectra. Individual percent variances: PC1 70; PC2 15. Solvent vapors: acetone (●), 1-propanol (□), 2-propanol (◇), benzene (△), cyclohexane (○), chloroform (■), dichloromethane (◆), water (▲), methanol (▼), ethanol (▽), and nitrogen (—).

Table 1. Rf Values for Array **I** with Intervening Acetone Exposures[a,b]

	methanol	dichloromethane	acetone	benzene	ethanol	chloroform	1-propanol	2-propanol	cyclohexane
dichloromethane	4.97								
acetone	16.6	8.85							
benzene	8.71	8.54	8.81						
ethanol	4.40	6.32	10.8	1.39					
chloroform	7.02	8.32	2.28	0.723	1.21				
1-propanol	4.46	5.21	8.46	5.20	0.510	2.87			
2-propanol	8.19	6.84	5.92	2.44	4.50	1.62	5.72		
cyclohexane	16.4	9.14	3.14	5.89	12.3	1.92	13.6	6.85	
water	4.03	7.35	11.5	5.45	1.43	3.52	2.45	4.12	12.1

[a] Array maintained at a constant temperature of 22 °C. [b] These data previously reported in graphical format in ref 15.

of the sensor array to differentiate between solvent vapor pairs as the temperature maximum of the temperature program is increased. The statistics show a meaningful decrease in the number of unresolved pairs along with an improvement in the other statistical descriptors. This effect appears to maximize with the 80 °C temperature program. When a 100 °C temperature program is applied, the resolution between many of the adjacent solvent vapor pairs is degraded to nearly the level of the room-temperature data. This effect is caused by a gradual decrease in the emission intensity of **3** due to the unintended heat transfer from the thermistors heating **1** and **2** when the 100 °C temperature program is run many successive times. The nitrogen "background" spectrum of **3** decreases ~15% over the span of 80 heating/solvent exposure cycles and is more erratic when the temperature program reaches 100 °C relative to the 50 °C or the 80 °C data. Additionally, if the data from **3** are dropped from the array and PCA is performed on the remaining data generated by **1** and **2** at 80 and 100 °C, the statistical results improve markedly at 100 °C while they worsen at 80 °C (see Table 3). These data support the premise that, at 100 °C, it is the gradual decomposition of **3** that decreases the discriminating power of the array, while at 80 °C, a more stable temperature for **3**, its presence enhances the effectiveness of the array.

On the basis of these results, we decided to replace **3** with **4** to form a new array designated as array **II**. Although **4** has a response less orthogonal to **1** and **2**, in comparison to **3**, it is much more thermally stable. This allows the entire array to be heated during the temperature programming step, a simplification that facilitated some additional interesting experiments. In this case, the three compounds were deposited onto a flexible foil heater and placed in the three-channel array sensor flow cell. When 25 V ac was applied across the leads of the flexible foil heater, the temperature at its surface quickly (<30 s) increased to 75−80 °C, at which time the voltage was turned off and the

Table 2. Rf Values for Array **I** with an Intervening Temperature Programming Cycle[a]

	methanol	dichloromethane	acetone	benzene	ethanol	chloroform	1-propanol	2-propanol	cyclohexane
dichloromethane	22.3								
acetone	41.0	30.0							
benzene	11.3	16.9	8.51						
ethanol	16.3	35.0	22.7	4.51					
chloroform	28.7	24.7	18.7	1.39	6.51				
1-propanol	6.43	33.4	17.7	5.40	6.12	9.43			
2-propanol	11.9	19.3	19.3	2.42	6.27	3.68	4.79		
cyclohexane	13.7	12.4	1.83	4.99	7.23	6.59	8.60	6.25	
water	7.33	20.3	22.7	5.00	6.05	9.28	1.74	6.29	8.66

[a] Only **1** and **3** are heated, ramped up to 80 °C, and then cooled to 25 ± 1 °C before acquiring spectra.

Table 3. Statistical Results with Array **I** and Different Types of Temperature Programming

	temperature (°C)					
	25[a]	50[b]	80[b]	100[b]	80[b,c]	100[b,c]
mean rf	5.5	11	13	8.1	13	8.9
min rf	0.56	0.47	1.4	0.47	1.4	1.6
max rf	13	41	41	21	4.6	22
no. of rf <3.75	14	5	5	14	9	8
no. of rf >3.75	31	40	40	31	36	37

[a] Constant temperature. [b] Ramp up to indicated temperature and then cool to 25 ± 1 °C before acquiring spectra. [c] Eliminate **3** data from PCA.

Table 4. Statistical Results with Array **II** and Different Types of Temperature Programming

	temperature (°C)			
	22[a]	50[a]	80[b]	80[b,c]
mean rf	9.9	6.7	11	13
min rf	0.63	1.1	0.53	2.2
max rf	59	22	54	46
no. of rf <3.75	13	13	7	6
no. of rf >3.75	32	32	38	39

[a] Constant temperature. [b] Ramp up to indicated temperature and then cool to 25° ± 1 °C before acquiring spectra. [c] N_2 stream dried with liquid N_2.

heater was allowed to cool back to room temperature. The results of these experiments are described in Table 4.

Comparing the results at 80 °C for array **I** (Table 3) to array **II** (Table 4) brings up several points that deserve comment. First, the statistical descriptors are fairly similar between the two arrays, with **I** producing a little more discriminating power for this solvent set compared to array **II**. Even though the individual compounds on **II** are not as orthogonal in their response to this solvent vapor set as **I**, **II** still does moderately well by compensating with a more reproducible spectral pattern across all three channels. Figure 4 demonstrates the more orthogonal response of array **I** (**1**−**3**) relative to **II** (**1**, **2**, **4**) for methanol vapor exposures relative to "background" nitrogen exposures. Figure 4 also highlights the greater reproducibility achieved with **II** relative to **I** for methanol vapor exposures. The reproducibility of **I** appears to suffer mostly due to the slow thermal decomposition of **3**, even using an 80 °C temperature program.

The response of **II** at a constant elevated temperature of ∼50 °C on a flexible foil heater was also studied. This temperature

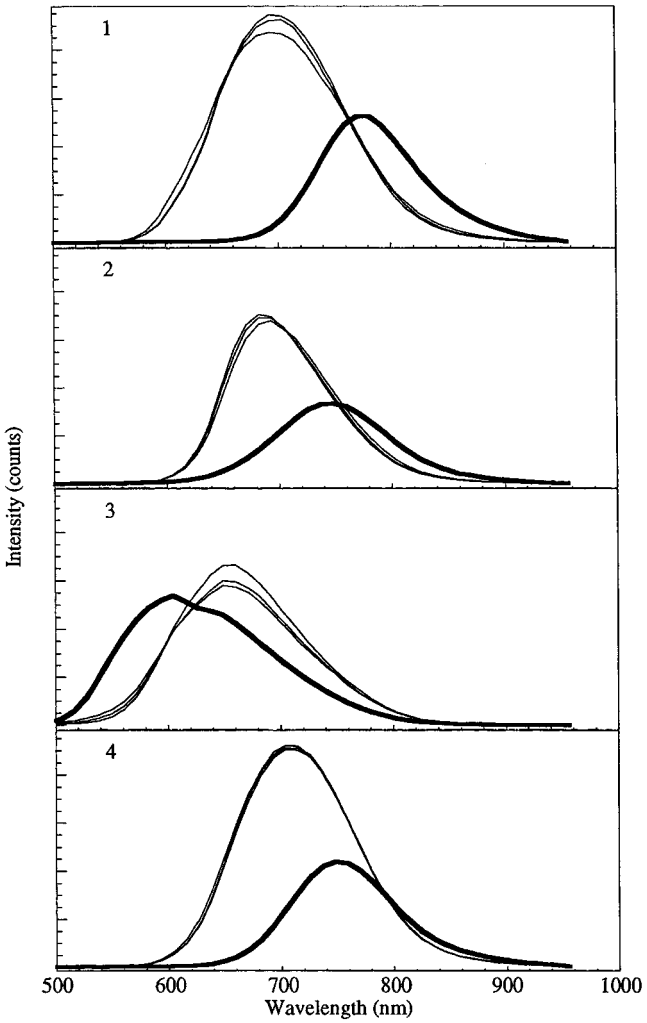

Figure 4. Luminescence spectra of **1**−**4** under methanol vapor (−) and nitrogen (—) acquired between a series of solvent exposures at 25 ± 1 °C after a temperature programming step to 80 °C during the nitrogen cycle. The nitrogen spectrum is an average of the four spectra acquired before the displayed methanol vapor spectra.

was achieved by placing 15 V dc across the leads of the heater. The thermocouple in the cell indicated that the temperature equilibrated at ∼48 ± 2 °C during the course of the experiment. Under these conditions, the spectral changes that occurred in the presence of the various solvent vapors were much less pronounced than at constant room temperature (22 °C); however, the reproducibility of the spectra was much better at the constant elevated

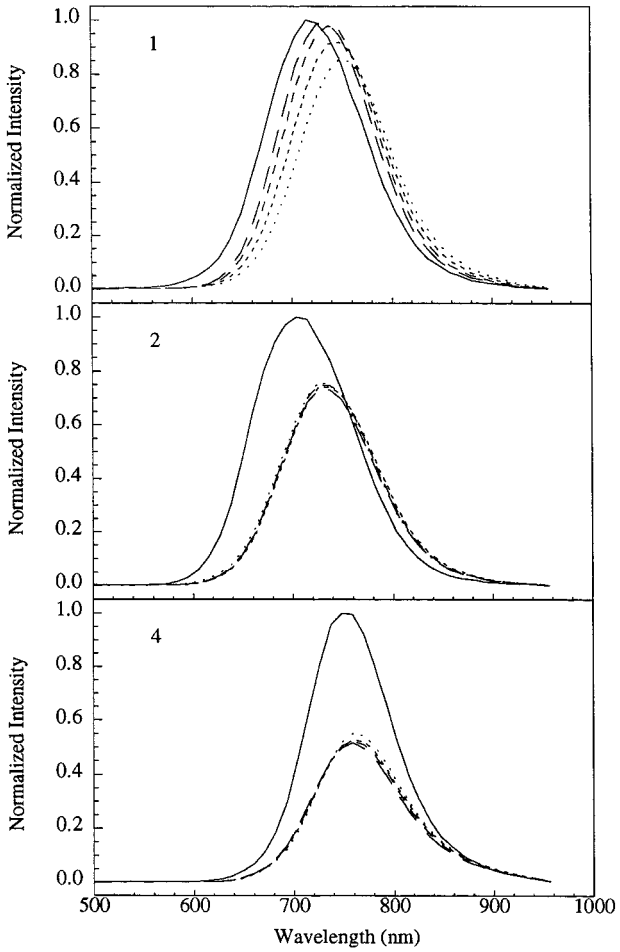

Figure 5. Luminescence spectra of array **II** (**1**, **2**, **4**) under saturated benzene vapor with varying degrees of humidity present. Humidity increases in the following order: ··· < - - - < **- - -** < **- - -**; the solid line is the spectrum at 100% humidity with no benzene present. Spectra acquired at 25 ± 1 °C after a temperature programming step to 80 °C during the nitrogen cycle. Each spectrum is an average of four cycles under each of the humidity levels studied.

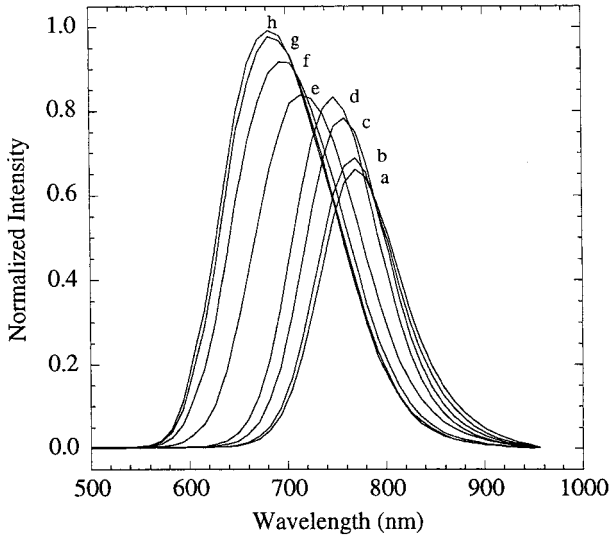

Figure 6. Luminescence spectra of **1** under varying concentrations of methanol vapor. Spectra acquired at 25 ± 1 °C after a temperature programming step to 80 °C during the nitrogen cycle. Each methanol spectrum is an average of three or four cycles while the nitrogen spectrum (a) is the average of all nitrogen backgrounds obtained (*N* = 27). Concentrations (percent saturation): a, 0; b, 1; c, 6; d, 11; e, 22; f, 54; g, 78; h, 100.

temperature of 50 °C, resulting in clusters that were tighter at 50 °C relative to 22 °C but also much closer together. In the end, the degree of differentiation appears to be nearly the same due to the opposite effect of these two factors.

The reasons for the success of the temperature programming protocol were investigated. Early on we observed that careful removal of background water vapor levels in the compressed nitrogen gas stream used between exposures seemed to slightly improve the reproducibility, and thus the discriminating power, of the array. As seen in Table 4, a slight improvement in the statistical descriptors for the 80 °C temperature programming protocol results if dry nitrogen gas was used as a carrier instead of compressed nitrogen. Therefore, it seemed reasonable that variations in water vapor contamination, present to some degree in all solvents, were at least partially mitigated by temperature programming. To further investigate this premise, a series of experiments were performed with benzene vapor, an analyte that generally gives the most scattered clusters in PC space. Array **II** was exposed repeatedly to benzene vapor after the array had been extensively dried by exposure to dry nitrogen for 2 h. A cycle consisted of exposure to nitrogen while the 80 °C temperature program was run followed by cooling to 25 ± 1 °C, diversion of the nitrogen through benzene solvent, and finally acquisition of an equilibrated luminescence spectrum. As seen in Figure 5, a series of consecutive exposures of benzene vapor to **II** under various levels of background humidity led to mostly reproducible responses from **2** and **4** but an obviously changing response from **1**. At the end of this experiment, the array was exposed to nitrogen saturated with water vapor. The spectra acquired under water vapor are also included in Figure 5. Note that **2** and **4** showed markedly different responses to saturated water vapor relative to their benzene responses; however, **1** only changed slightly. In addition, to recover the luminescence spectra obtained under benzene vapor in dry nitrogen after a water vapor exposure, a heating cycle was required followed by a ~2-h exposure to dry nitrogen. This indicates that even this heating cycle may not remove all the residual water in the sensor materials. On the basis of these results, **1** appears to be the most sensitive to low background humidity levels. We also conclude that the equilibrium constant for the inclusion of water into sensor **1** is likely much larger than the corresponding equilibrium constant for benzene and probably other hydrocarbons as well. This is in line with expected trends in the strength of hydrogen bonding compared with dispersion forces between the chromophore and the solvent guest. The sensitivity of some of these sensor materials to background humidity levels raises an issue that must be successfully addressed if these compounds are to be used as a practical sensor array. Finally, even though these studies suggest different humidity levels are a major source of noise in these systems, we have not eliminated the possibility that other high-boiling contaminants present in the various solvents could also be problematic. Temperature programming between solvent vapor exposures is expected to partially mitigate this potential problem as well.

The ability of array **I** to differentiate and detect analyte gases at concentrations less than saturation was also investigated.

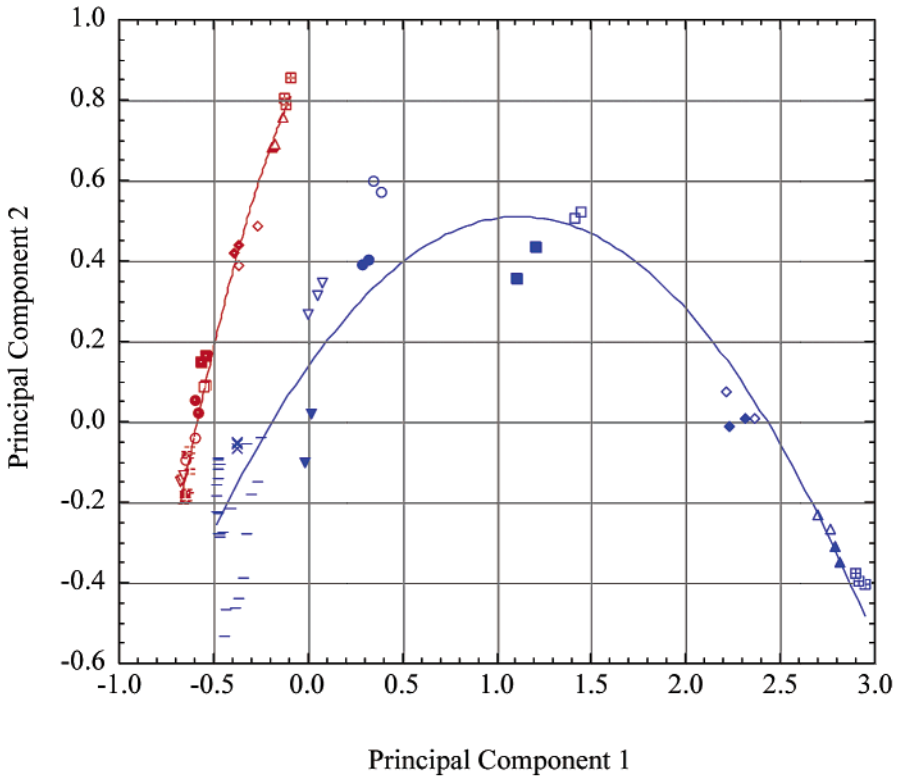

Figure 7. PC2 vs PC1 score plot from PCA of luminescence spectra of array **I** with varying acetone (red) and methanol (blue) concentrations in nitrogen. Filled points were used to plot the ascending concentration data, and open points were used for the descending concentration data. The red and blue lines are visual guides for the methanol and acetone data, respectively. Only **1** and **2** are directly heated by ramping up to 80 °C and then cooling to 25 ± 1 °C before acquiring spectra. Individual percent variances: PC1 84; PC2 8.2. Approximate concentrations (percent saturation): 0 (−), 1 (×), 5 (▽), 10 (○), 20 (□), 50 (◇), 75 (△), and 100 (⊞); please see Supporting Information for exact concentrations.

Saturated methanol and acetone vapors were diluted with nitrogen gas and passed over the array elements in separate experiments. These particular solvent vapors were chosen as they represent a vapor that causes major spectral changes at saturation, i.e., methanol, and a vapor that induces only mild spectral changes at saturation, i.e., acetone. Figure 6 shows an example of the type of data acquired in these experiments for methanol exposure to **1**. Note that not only does the intensity vary but the spectrum also blue shifts as the concentration of methanol is increased in a process that is at least biphasic. Because an isosbestic point was not obtained, the intensity at one wavelength as a function of concentration does not extract all the information in the data set. Therefore, the luminescence spectra collected in the two experiments were pooled and analyzed by PCA. Figure 7 shows the first two principal components of the analysis. As expected, the methanol vapor data covered a much larger portion of PC space than acetone due to the more extensive spectral changes methanol evokes. Data points collected ascending and descending the concentration scale are nearly identical, so little or no hysteresis is associated with the concentration response of the sensor array with respect to methanol or acetone exposure. The nitrogen background for the acetone data set was slightly different from the nitrogen background for the methanol data set (rf = 5.9), probably due to the difference in water contamination in acetone relative to methanol. Apparently, the temperature programming does not remove all the residual water from the sensor materials; therefore, a different steady-state background level of water is achieved in acetone relative to methanol. The rf analysis of the data also indicates that the entire acetone concentration range was resolved from every point in the methanol concentration range using the criterion that neighboring clusters having rf values greater than 3.75 can be differentiated (see Supporting Information).

A detection limit was estimated using the standard deviation of the nitrogen PC coordinates (blank) along vectors to neighboring concentration clusters (signal) in a technique similar to the rf calculation. Invoking a typical "standard deviation of the blank times three" criterion for the detection limit, a minimal detectable distance from the centroid of the nitrogen cluster was determined for acetone and methanol. Based on this approach, the detection limit for acetone was at 12% saturation (75 g/m^3) using array **I** with the specified temperature programming protocol. Methanol gave a lower detection limit at 3% (6 g/m^3).

CONCLUSIONS

We have further demonstrated the potential analytical applications of platinum(II) double salt materials in cross-reactive sensor arrays. Applying a temperature cycle between solvent exposures greatly improved the ability of the arrays studied to differentiate between a set of 10 solvent vapors. Care must be taken in the choice of the maximum temperature in the heating cycle as some of the platinum(II) double salt materials studied here tend to decompose at elevated temperatures. In addition, some of these materials were also sensitive to background water vapor levels that reduced the reproducibility of the luminescence spectra obtained for a given solvent vapor. A practical cross-reactive sensor array of platinum(II) double salt materials may be possible if they

are designed at the molecular level to be thermally stable and insensitive to low levels of water vapor contamination. The nonlinear response observed for some of the vapors studied is also a complicating factor that will need to be addressed. Synthetic experiments designed to produce new compounds that meet these additional requirements are underway in our laboratory. Finally, concentration studies comparing acetone and methanol have shown for the first time that arrays of platinum(II) double salt materials can be used to differentiate two solvent vapors over their entire detectable concentration range.

ACKNOWLEDGMENT

This work is supported by the University of Washington Center for Process Analytical Chemistry (CPAC) and the National Science Foundation, most recently under Grant CHE-9307837. S.M.D. acknowledges sabbatical support from the Howard Hughes Medical Institute and Carleton College.

SUPPORTING INFORMATION AVAILABLE

Synthesis and characterization details for **2**−**4**, isocyanide ligands, and ligand precursors. Additional evidence for the formulation of **4**. Method used to correct percent saturation values for the uptake of solvent vapor with the partitioning flow apparatus. PC3 vs PC1 plots for the data presented in Figures 2, 3, and 7. Loadings plots for the data presented in Figures 2, 3, and 7. Rf table for the methanol and acetone concentration data. This material is available free of charge via the Internet at http://pubs.acs.org.

Received for review December 11, 2001. Accepted February 15, 2002.

AC011255D